

## Characterizing Astrophysical Binary Neutron Stars with Gravitational Waves

XING-JIANG ZHU (朱兴江)<sup>1,2</sup> AND GREGORY ASHTON (艾格瑞)<sup>1,2</sup>

<sup>1</sup>*School of Physics and Astronomy, Monash University, Clayton, VIC 3800, Australia*

<sup>2</sup>*OzGrav: Australian Research Council Centre of Excellence for Gravitational Wave Discovery, Clayton, VIC 3800, Australia*

### ABSTRACT

Merging binary neutron stars are thought to be formed predominantly via isolated binary evolution. In this standard formation scenario, the first-born neutron star goes through a recycling process and might be rapidly spinning during the final inspiral, whereas the second-born star is expected to have effectively zero spin at merger. Based on this feature, we propose a new framework for the astrophysical characterization of binary neutron stars observed from their gravitational wave emission. We further propose a prior for the dimensionless spin magnitudes of recycled neutron stars, given by a gamma distribution with a shape parameter of 2 and a scale parameter of 0.012, from radio pulsar observations of Galactic binary neutron stars. Interpreting GW170817 and GW190425 in the context of the standard formation scenario, we find positive support for a spinning recycled neutron star (with a spin tilt angle  $\lesssim 60^\circ$ ) in GW190425 with a Bayes factor of 6, whereas the spin of the recycled neutron star in GW170817 is small and consistent with our prior. We measure the mass of the recycled (slow) neutron star in GW170817 and GW190425 to be  $1.34_{-0.09}^{+0.12}$  ( $1.38_{-0.11}^{+0.11}$ )  $M_\odot$  and  $1.64_{-0.11}^{+0.13}$  ( $1.66_{-0.12}^{+0.12}$ )  $M_\odot$ , with 68% credibility, respectively. The mass ratio of GW170817 (GW190425) is constrained to be between 0.79 (0.80) and 1, with 90% credibility.

*Keywords:* Gravitational waves, Neutron stars, Bayesian statistics

### 1. INTRODUCTION

The ground-based gravitational-wave interferometers Advanced LIGO (Aasi et al. 2015) and Advanced Virgo (Acernese et al. 2015) have discovered dozens of compact binary coalescence events (Abbott et al. 2019a, 2020a,b; Abbott et al. 2020) and numerous candidates<sup>1</sup>. These include binary black holes, binary neutron stars (BNS), and possibly neutron star-black hole mergers<sup>2</sup>, which are revolutionizing our understanding of the Universe.

Current gravitational-wave inference methods (Veitch et al. 2015; Biwer et al. 2019; Ashton et al. 2019) label the two merging compact objects as primary and secondary, with corresponding masses  $m_1 \geq m_2$ . In this work, we propose a new astrophysically motivated parameterization for BNS using a *recycled* and *slow* labelling scheme. Assuming standard formation via isolated binary evolution (e.g., Tauris et al. 2017), the two

components of the BNS system have distinct properties. The first-born neutron star (NS) is expected to undergo a recycling process where it gets spun up by accreting matter and angular momentum from its companion star (prominently during the case BB Roche-lobe overflow). The end product is a recycled NS, with a spin period of order 10 to 100 ms and very low spin-down rate. The second-born NS, on the other hand, is “normal”: it spins down quickly, in  $\lesssim 10$  Myr from a birth spin period of tens of ms to  $\mathcal{O}(1)$  s. For gravitational-wave analysis, the second born NS is effectively nonspinning during the final inspiral, hence termed as the slow NS. In the astrophysical parameterization, the mass (dimensionless spin magnitude) of the recycled and slow NS is denoted as  $m_r$  ( $\chi_r$ ) and  $m_s$  ( $\chi_s$ ), respectively. In Section 2, we propose an astrophysical prior with  $\chi_r > 0$  and  $\chi_s = 0$ , and we do not impose any ordering on  $m_r$  and  $m_s$ .

There are presently 17 known Galactic BNS systems<sup>3</sup> with reported total masses from radio pulsar observa-

Corresponding author: Xing-Jiang Zhu  
zhuxingjiang@gmail.com

<sup>1</sup> <https://gracedb.ligo.org/superevents/public/O3/>

<sup>2</sup> The latest published event, GW190814, contains the lightest black hole or heaviest neutron star (Abbott et al. 2020b).

<sup>3</sup> There are potentially another two, but with no mass measurement and not expected to merge within a Hubble time (see Table 2 of Tauris et al. 2017).

tions; 12 of them have component masses measured (see [Zhu et al. 2018](#), and references therein). Among these binaries, the Double Pulsar (J0737–3039A/B) is unique with both NS being observed as radio pulsars ([Burgay et al. 2003](#); [Lyne et al. 2004](#)): one is recycled with a spin period ( $P$ ) of 22.7 ms and a spin-down rate ( $\dot{P}$ ) of  $1.76 \times 10^{-18}$ , and the other is slow with a spin period of 2.8 s and a spin-down rate of  $8.92 \times 10^{-16}$ . It is expected to merge in 86 Myr. There are another nine BNS that will merge within a Hubble time. All but one observed pulsars in these BNS are recycled, with spin periods from 17 to 76.5 ms, and spin-down rates from  $1.6 \times 10^{-19}$  to  $8.6 \times 10^{-18}$ . The exception is PSR J1906+0746, which is a young pulsar with a spin period of 144 ms. It is spinning down quickly ( $\dot{P} = 2 \times 10^{-14}$ ) and will become a slow pulsar when merging with its companion in 0.3 Gyr ([van Leeuwen et al. 2015](#)).

The majority of known Galactic BNS are found in the Galactic disk and can be described via the standard formation scenario (e.g., [Tauris et al. 2017](#)). Among 10 merging BNS in the Galaxy, PSR B2127+11C is the only exception, being found in the globular cluster M15 ([Anderson et al. 1990](#)). [Phinney & Sigurdsson \(1991\)](#) and [Prince et al. \(1991\)](#) suggested that the original stellar companion of PSR B2127+11C might be replaced by another NS through a dynamical encounter, which also resulted in the ejection of the BNS to the outskirts of M15. It was estimated that the BNS merger rate from globular clusters similar to M15 can account for a significant fraction ( $\sim 10\text{--}30\%$ ) of observed short gamma-ray bursts ([Grindlay et al. 2006](#); [Lee et al. 2010](#)). However, [Ye et al. \(2020\)](#) found that dynamical interactions in globular clusters are dominated by black holes and thus make a negligible contribution to the overall BNS merger rate (see also [Belczynski et al. 2018](#)). Therefore, it is generally believed that the BNS merger rate inferred from LIGO/Virgo observations is dominated by the standard isolated binary evolution channel ([Mapelli & Giacobbo 2018](#); [Neijssel et al. 2019](#)), although see [Andrews & Mandel \(2019\)](#) for speculation of a dynamical origin for several Galactic-disk BNS with similar orbital characteristics to B2127+11C.

[Farrow et al. \(2019\)](#) analyzed mass measurements of Galactic BNS and found modest evidence for distinct distributions of  $m_r$  and  $m_s$ , and a bimodal distribution of  $m_r$ . These features might be due to different supernova explosion mechanisms ([Schwab et al. 2010](#); [Pejcha et al. 2012](#)), or the recycling process (but probably to a much lesser extent, see, e.g., [Tauris et al. 2017](#)). [Farrow et al. \(2019\)](#) demonstrated that dozens of new BNS observations, which are achievable with future observing runs of Advanced LIGO/Virgo and ongoing radio pulsar

surveys in  $\lesssim 5$  years, are required to draw firm conclusions. In this work, we make use of observational properties of Galactic BNS systems and propose an astrophysical prior on the spin ( $\chi_r$ ) of recycled NS. This will allow us to probe distributions of  $m_r$  and  $m_s$  through gravitational-wave observations.

The remainder of this paper is organized as follows. In Section 2, we derive an astrophysical prior on  $\chi_r$ . In Section 3, we apply the new prior to GW170817 ([Abbott et al. 2017](#)) and GW190425 ([Abbott et al. 2020](#)) and present our findings. Last, we summarize and discuss future prospects in Section 4.

## 2. AN ASTROPHYSICAL PRIOR ON NEUTRON STAR SPINS

We now establish an astrophysical prior on the dimensionless spin magnitudes,  $\chi_r$ , of the recycled NS in BNS systems, as measured in the final binary inspiral. Following [Zhu et al. \(2018\)](#), we extrapolate from the observed properties of 10 Galactic BNS to a representative population of BNS, each characterized by  $m_r$ ,  $m_s$ , initial orbital period  $P_b$  and eccentricity,  $P$  and  $\dot{P}$  of the recycled NS at the birth of second NS. Observationally, the spin periods of recycled pulsars in Galactic-disk BNS systems appear to be correlated with their orbital periods (see Figure 8 in [Zhu et al. 2018](#)). To generate our birth BNS population, we make use of the following empirical  $P$ - $P_b$  correlation ([Tauris et al. 2015, 2017](#))

$$P = (36 \pm 14) \text{ ms } (P_b/\text{days})^{0.4}. \quad (1)$$

Equation (1) suggests that binaries born with tighter orbits tend to contain faster-spinning recycled NS, which can be (qualitatively) attributed to a longer recycling process (see [Tauris et al. 2017](#), for details). To obtain the distribution of  $P$  at merger, we follow the spin-down evolution of each recycled NS in our population from the birth of the BNS to binary merger, adopting a magnetic dipole braking model. The initial spin-down rate is determined by assigning a log-normal distribution of magnetic field strength that covers the range of measurements for Galactic BNS, given a NS equation of state or radius parameter. The magnetic field strength is assumed to be constant from binary birth to merger. Whereas magnetic field decay might occur for young NS ([Goldreich & Reisenegger 1992](#)) or for NS undergoing the recycling process ([Taam & van den Heuvel 1986](#); [Romani 1990](#)), it is thought to be unlikely for recycled NS such as millisecond pulsars ([Bransgrove et al. 2018](#)). More details on the methodology and prescriptions of the BNS population can be found in [Zhu et al. \(2018\)](#).

The definition of  $\chi \propto I/(m^2 P)$  means that there are three ingredients in the distribution of  $\chi$ : 1) the distribution of spin periods ( $P$ ), 2) the distribution of masses

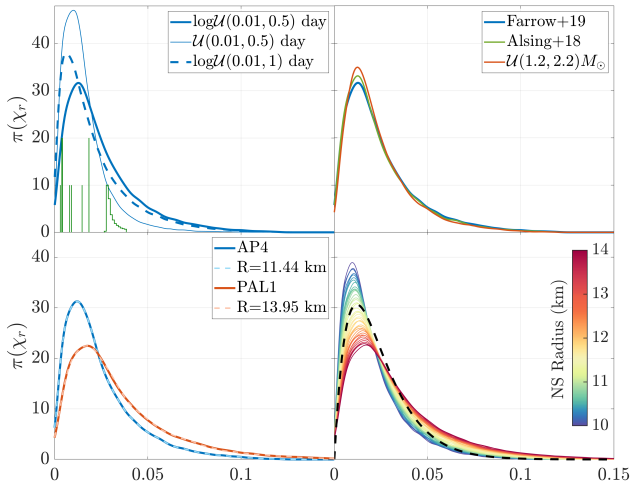


**Figure 1.** The probability distribution of the dimensionless spin magnitudes  $\pi(\chi_r)$  of recycled NS in BNS systems. *Top-left:* different initial binary orbital period distributions ( $\mathcal{U}$  – Uniform distribution, and  $\log\mathcal{U}$  – Uniform distribution in a  $\log_{10}$  scale), along with expected  $\chi$  during merger for 9 recycled pulsars in merging Galactic BNS (green lines, scaled to coordinate height of 10 for each NS – a height of 20 indicates two pulsars having identical  $\chi$  at merger). *Top-right:* different mass distributions – Farrow+19 (Farrow et al. 2019), Alsing+18 (Alsing et al. 2018) and Uniform between 1.2 and  $2.2 M_{\odot}$ . *Bottom-left:* two NS equations of state (AP4 and PAL1) and under the assumption that all NS have the same radius ( $R=11.44$  km and  $13.95$  km). Note that there exist subtle differences between using a equation of state model and a single NS radius parameter; solid and dashed lines precisely overlap as a result of curve smoothing. *Bottom-right:* distribution of  $\chi_r$  for a range of NS radii from 10 to 14 km (colored lines), and the gamma distribution with a shape parameter of 2 and a scale parameter of 0.012 (black dashed line). We note that our spin distribution model shown here is qualitatively similar to more sophisticated population synthesis models (e.g., Chattopadhyay et al. 2020).

( $m$ ), and 3) the equation of state, which, together with  $m$ , determines the moment of inertial ( $I$ ). Below, we describe a model for the distribution of  $\chi_r$  that takes into account uncertainties in these three ingredients<sup>4</sup>.

In Figure 1, we show the effect of different initial orbital period ( $P_b$ ) distributions (top-left panel), mass distributions (top-right panel), and the NS equation of state (bottom two panels) on the distribution of  $\chi_r$ . In our fiducial model, we assume a log-uniform distribution of  $P_b$  between 0.01 and 0.5 days. In comparison, the orbital periods of 10 Galactic BNS that are capable of merging within a Hubble time range from 0.078 to 0.421

days. By applying the  $P$ - $P_b$  correlation down to an orbital period of 0.01 days, the fastest birth spin period is about 5 ms. Overall, around 10% of recycled NS have  $P \lesssim 10$  ms at birth in our population. This makes our model conservative since theoretical modelling of standard BNS formation suggests that the first-born NS is usually only mildly recycled; Tauris et al. (2015) found a fastest spin period of 11 ms assuming an accretion efficiency of three times the Eddington limit during the case BB Roche-lobe overflow.

Based on measurements of Galactic BNS (Farrow et al. 2019), we adopt a two-Gaussian distribution of  $m_r$ , peaking at  $1.34$  and  $1.47 M_{\odot}$ , with width of  $0.02$  and  $0.15 M_{\odot}$  and weight of  $0.68$  and  $0.32$ , respectively; the distribution of  $m_s$  is uniform between  $1.16$  and  $1.42 M_{\odot}$ . The distribution of  $m_s$  is only used for the merger-time calculation and we find its functional form has no impact on our result. Our fiducial choice of equation of state is AP4 (Lattimer & Prakash 2001).

In the top-left panel of Figure 1, we show the result for two alternative distributions of  $P_b$ : a) uniform between 0.01 and 0.5 days (thin solid line), and b) log-uniform between 0.01 and 1 days (thick dashed line). In comparison to our fiducial model (thick solid line), both a) and b) result in a smaller fraction of fast-spinning NS, because recycled NS spin more slowly at birth in long- $P_b$  binaries and the spin-down time is longer (meaning smaller residual spins at merger). Even though a) and b) may appear to provide a better fit to Galactic BNS (shown as green lines), we choose our fiducial model for two reasons. First, it compensates the selection effect that short- $P_b$  BNS are more difficult to detect in radio pulsar surveys because of severe Doppler smearing of pulse signals and their short lifetimes. Second, it results in a conservative prior by allowing relatively large spins for gravitational-wave parameter estimation.

In the top-right panel of Figure 1, we show the spin distribution for three mass models. In addition to the model of Farrow et al. (2019), we also consider: 1) the two-Gaussian model of Alsing et al. (2018) fitted to mass measurements of NS in all binaries, peaking at  $1.34$  and  $1.80 M_{\odot}$ , with width of  $0.07$  and  $0.21 M_{\odot}$  and weight of  $0.65$  and  $0.35$ , respectively; and 2) a uniform distribution between  $1.2$  and  $2.2 M_{\odot}$ . It is apparent that the spin magnitude distribution is insensitive to the mass model. In the bottom-left panel, we show the distribution of  $\chi_r$  for two NS equations of state – AP4 and PAL1, as investigated in Zhu et al. (2018), and assuming that all NS have the same radius ( $11.44$  km and  $13.95$  km, respectively). It can be seen that the effect of equation of state is completely captured by the radius parameter.

<sup>4</sup> A more natural choice of prior would be on  $P$ , so that the mass distribution and NS equation of state can be simultaneously inferred with a population of events (e.g., Wysocki et al. 2020).

In the bottom-right panel of Figure 1, we show the spin distribution (depicted in different colors) for a range of NS radius from 10 to 14 km – a plausible range allowed by current gravitational-wave and pulsar observations (Landry et al. 2020). As an arbitrary fit to the group of colored curves, the black dashed curve is given by the gamma distribution with a shape parameter of 2 and a scale parameter of 0.012. We propose this gamma distribution to be used as an astrophysical prior on  $\chi_r$  in gravitational-wave data analysis. Once dozens or more BNS events are detected, we may be able to update the prior to reveal information encoded in the spin distribution as shown in Figure 1 (see also Zhu et al. 2018). For the slow NS, it is reasonable to set  $\chi_s = 0$ ; a spin period of 3 s (i.e., that of the slow pulsar in the Double Pulsar system) corresponds to  $\chi_s \approx 10^{-4}$ , which is effectively zero for gravitational-wave measurements.

Spin effects measurable in gravitational waves are represented by two parameters (e.g., Abbott et al. 2019b): 1) the effective spin parameter  $\chi_{\text{eff}}$ , which is the mass-weighted combination of spins along the orbital angular momentum vector  $\mathbf{L}$ ; 2) the effective spin-precession parameter  $\chi_p$ , which quantifies the spin components perpendicular to  $\mathbf{L}$ . By setting  $\chi_s = 0$ , we have  $\chi_{\text{eff}} = m_r \chi_r \cos \theta / (m_r + m_s)$ , and  $\chi_p = \chi_r \sin \theta$ , where  $\theta$  is the spin tilt angle of the recycled NS with respect to  $\mathbf{L}$ . Next, we summarize our prior knowledge of  $\theta$  from pulsar observations and binary evolution theory.

By measuring the pulse profile variations induced by spin precession, the spin tilt angle is constrained for four recycled pulsars in Galactic BNS: PSR J0737–3039A  $\theta < 3.2^\circ$  (Ferdman et al. 2013), PSR B1913+16  $\theta = 18 \pm 6^\circ$  (Kramer 1998), PSR B1534+12  $\theta = 27 \pm 3^\circ$  (Fonseca et al. 2014), PSR J1756–2251  $\theta < 34^\circ$  (Ferdman et al. 2014). From a binary evolution perspective, the spin axis of recycled NS gets aligned with orbital angular momentum during the recycling process (Hills 1983; Bhattacharya & van den Heuvel 1991), therefore the spin tilt angle is generally related to the supernova kick imparted on the second-born NS directed out of the orbital plane. Bailes (1988) considered a range of BNS progenitors for PSR B1913+16 and a Rayleigh distribution with a scale parameter of  $150 \text{ km s}^{-1}$  for the kick velocity, and showed that  $\theta \lesssim 60^\circ$ . This is consistent with observations of four Galactic BNS mentioned above and implies large spin tilt angles are unlikely *a priori*.

### 3. GW170817 AND GW190425

Adopting our astrophysical parameterization of the masses and spins ( $m_r, m_s, \chi_r, \chi_s$ ) and the spin prior derived in Section 2, we reanalyze the two BNS merger events detected by LIGO/Virgo: GW170817

and GW190425. We use the IMRPhenomPv2\_NRTidal waveform model, which includes an effective description of spin-precession and tidal effects (Hannam et al. 2014; Khan et al. 2016; Dietrich et al. 2017a; Dietrich et al. 2019). In our prior, the detector-frame binary chirp mass is uniform in  $[1.18, 1.21]$  ( $[1.48, 1.495]$ )  $M_\odot$  for GW170817 (GW190425) and the mass ratio is uniform in  $[0.125, 8]$ . Priors for other source parameters are identical to those used in the LIGO/Virgo discovery papers (Abbott et al. 2017, 2020); for GW170817, we fix the sky location to its host galaxy NGC4993 (Abbott et al. 2017a).

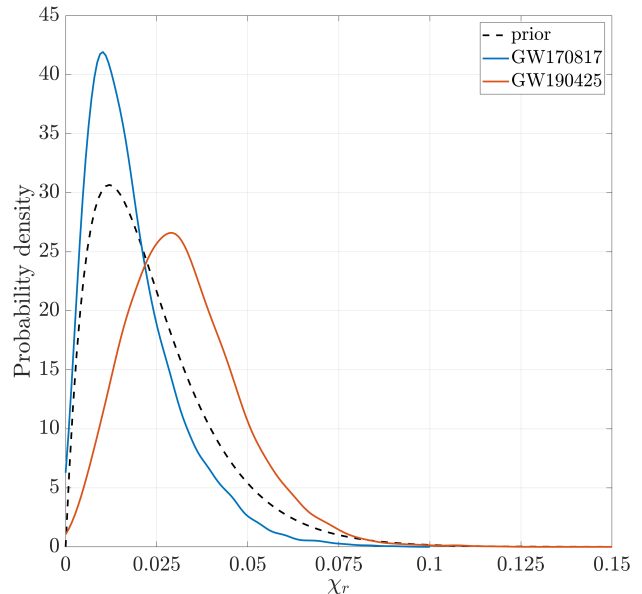


**Figure 2.** Posterior distributions of the dimensionless spin magnitudes ( $\chi_r$ ) of recycled NS in GW170817 and GW190425, derived under the astrophysical prior (black dashed line) and assuming aligned spins.

Assuming aligned spins, we obtain a Bayes factor of 6 (0.8) between the spinning and nonspinning hypothesis for GW190425 (GW170817). This implies weak evidence of NS spin in GW190425, and that the spin of the recycled NS in GW170817 is small. Figure 2 shows the posterior distributions of  $\chi_r$ , along with the prior. In accordance with Bayes factor results, the posterior of GW190425 moderately shifts toward larger spins, peaking at  $\chi_r = 0.03$  in comparison to 0.012 for the prior; for GW170817 the posterior is similar to the prior, only slightly shifting toward lower spins.

Assuming a uniform prior for  $\cos \theta$  between  $-1$  and  $1$  (i.e., random spin orientation), Figure 3 shows the posterior probability densities of  $\chi_r$  with respect to the orbital angular momentum  $\mathbf{L}$  for GW170817 and GW190425,

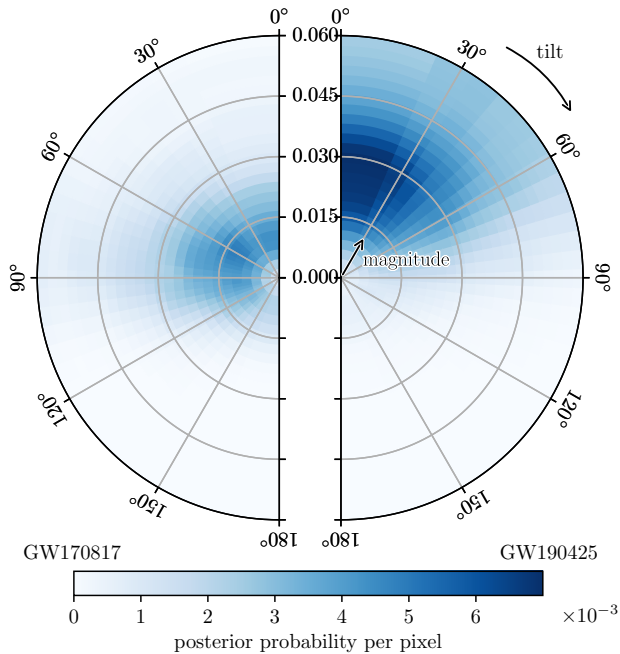


**Figure 3.** Posterior probability densities of  $\chi_r$  in GW170817 (left) and GW190425 (right), with respect to the orbital angular momentum  $\mathbf{L}$ . This is shown for the astrophysical spin prior using the IMRPhenomPv2\_NRTidal waveform at a reference frequency of 20 Hz. A tilt angle of  $0^\circ$  indicates alignment with  $\mathbf{L}$ .

on the left and right half-disk, respectively. We find the spin in GW170817 is only weakly constrained, disfavoring anti-alignment with  $\mathbf{L}$ , whereas the spin tilt angle can be constrained to be  $\lesssim 60^\circ$  for GW190425, being consistent with pulsar observations of Galactic BNS.

Figure 4 shows the joint posterior distributions of  $(m_r, m_s)$  for GW170817 and GW190425, along with 10 merging Galactic BNS (Farrow et al. 2019). We find both GW170817 and GW190425 are likely equal-mass binary mergers, consistent with previous results using the  $m_1 - m_2$  parameterization under the low-spin prior ( $\chi < 0.05$ ); see Figure 6 in Appendix B for details. We measure the mass of the recycled (slow) NS to be  $1.34^{+0.12}_{-0.09}$  ( $1.38^{+0.11}_{-0.11}$ )  $M_\odot$  and  $1.64^{+0.13}_{-0.11}$  ( $1.66^{+0.12}_{-0.12}$ )  $M_\odot$ , with 68% credibility, for GW170817 and GW190425, respectively. Re-ordering  $(m_r, m_s)$  into  $(m_1, m_2)$ , we obtain slightly improved constraints on the mass ratio (defined as  $q \leq 1$ ). For GW170817 (GW190425), our 90% credibility lower bound on  $q$  is 0.79 (0.80), in comparison to 0.73 (0.78) by LIGO/Virgo collaborations assuming the low-spin prior.

We find the mass ratio of the most asymmetric merging Galactic BNS, PSR J1913+1102, recently measured to be  $0.78 \pm 0.03$  (Ferdman et al. 2020), is largely inconsistent (at 92% credibility) with our posterior probab-

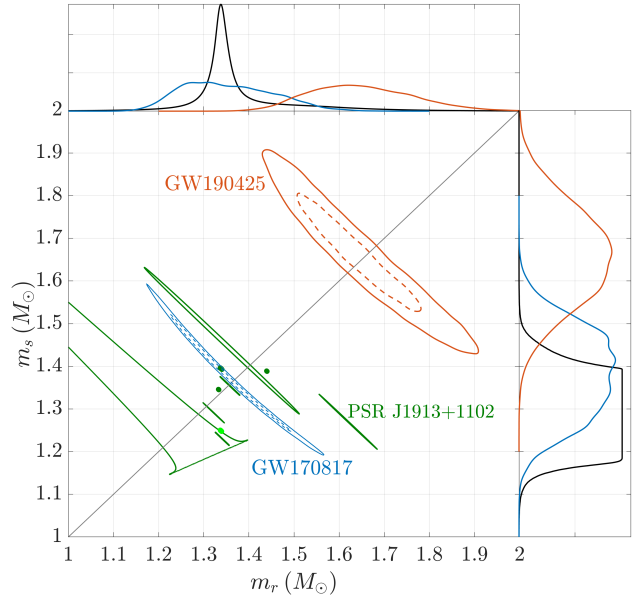


**Figure 4.** Posterior distributions of NS masses ( $m_r$  and  $m_s$ ) of GW170817 and GW190425, along with 10 merging Galactic BNS (green lines). Solid (dash) lines encompass 90% (50%) credible region. Due to high measurement precision, four Galactic BNS are indicated as dots in the figure. One-dimensional marginalized distributions are given in the small panels on the top and right; black curves illustrate the posterior predictive distributions based on the Galactic BNS population (Farrow et al. 2019), where  $m_r$  and  $m_s$  follows a two-Gaussian and uniform distribution, respectively.

ity distribution of GW170817. Our constraint on  $q$  for GW170817 disfavours a dynamical origin for the ejecta associated with the kilonova accompanying GW170817 at optical and near-infrared wavelengths (e.g., Dietrich et al. 2017b; Abbott et al. 2017b; Gao et al. 2017; Pankow 2018), and could lend support for alternative origins such as magnetar winds (Metzger et al. 2018) or accretion disk outflow (Siegel & Metzger 2018).

In the one-dimensional marginal distribution plots of Figure 4, we show as black lines the posterior predictive distributions of  $m_r$  and  $m_s$  derived in Farrow et al. (2019) for Galactic BNS systems. We find the measurements of  $m_r$  and  $m_s$  for GW170817 are fully consistent with the Galactic BNS model. The measured  $m_r$  in GW190425 is broadly consistent with the secondary peak (at  $1.47 M_\odot$  with a width of  $0.15 M_\odot$ ) of the Galactic model, and is similar to  $1.62 \pm 0.03 M_\odot$  of PSR J1913+1102 (Ferdman et al. 2020) – the most massive recycled pulsar in Galactic BNS systems. However, the measurement of  $m_s$  of GW190425 is inconsistent with the Galactic population ( $\lesssim 1.42 M_\odot$ ) at the 95% confidence level. We find such a tension is less severe than the  $5\text{-}\sigma$  discrepancy between the binary total mass of

GW190425 and the Galactic BNS population found in Abbott et al. (2020); note also the distance of its joint  $(m_r, m_s)$  posterior from other measurements along the equal-mass diagonal line in Figure 4. We expect future gravitational-wave observations of BNS mergers will either fill the gap in the  $(m_r, m_s)$  space shown in Figure 4, or confirm GW190425 as part of a distinct sub-population (Romero-Shaw et al. 2020).

#### 4. CONCLUSION

We propose a new parameterization for the study of gravitational waves from BNS mergers, which consist of a recycled NS and a slow (i.e., effectively nonspinning) NS as expected from the standard isolated binary evolution formation channel. Inspired by radio pulsar observations of  $\mathcal{O}(10)$  Galactic BNS systems, we derive a representative distribution for the dimensionless spin magnitudes of recycled NS, given by a gamma distribution with a shape parameter of 2 and a scale parameter of 0.012. Applying this distribution as an astrophysical prior, we find weak evidence of spin in GW190425 with a Bayes factor of 6. The spin tilt angle is  $\lesssim 60^\circ$ , being consistent with observations of Galactic BNS.

The proposed prior on NS spins also allows us to measure the masses of recycled and slow NS, directly linking to radio pulsar measurements of Galactic BNS. We find that both GW170817 and GW190425 are likely to be equal-mass mergers: both the recycled and slow NS masses are around  $1.35 M_\odot$  for GW170817, and around  $1.65 M_\odot$  for GW190425. Whereas the masses of GW170817 are fully consistent with the Galactic BNS population, we find the slow NS mass of GW190425 is significantly greater than those of Galactic BNS, although the inconsistency level (95%) is somewhat lower than the  $5\text{-}\sigma$  tension in terms of binary total mass. Future gravitational-wave measurements of NS masses will provide important insights into the existence of potential sub-populations of BNS.

We focus on BNS formed through the standard isolated binary evolution channel. While current merger-rate estimates suggest that nearly all BNS mergers should be formed via the standard channel, one detected event outside the astrophysical prior proposed in

this work would indicate a new origin. For example, in our prior,  $\chi \gtrsim 0.05$  is relatively rare (8%), which arises from the theoretical expectation that the first-born NS is only moderately recycled. However, a dynamically formed BNS could contain a fully recycled millisecond NS ( $\chi \sim 0.1 - 0.2$ ). If both NS were found to exhibit measurable spins, it would imply a dynamically formed BNS containing two recycled NS, or in case where one NS is non-recycled, it is probably born fast-spinning and still young ( $\ll 1$  Myr) at merger. We test these possibilities for GW190425 and find the data are not informative enough to distinguish them from the standard scenario; see Appendix A for details.

Finally, the astrophysical prior on NS spins proposed in this work will enable future gravitational-wave analyses of BNS mergers to determine whether or not recycled NS and slow NS follow different mass distributions. This will in turn have significant implications on supernova explosion mechanisms involved in BNS formation. Once dozens of BNS mergers are detected, such a prior will also enable the measurement of the typical spin tilt angle of the recycled NS, which encodes information about the magnitude of supernova kicks applied to the slow NS. A population of  $\mathcal{O}( > 100)$  detected events will update the prior and reveal information about NS equation of state, the distribution of initial BNS orbital periods, and potentially magnetic field decay (if exists) of recycled NS.

We thank Michael Zevin and He Gao for useful comments. X.Z is supported by ARC CE170100004, G.A is supported by ARC DP180103155. This research has made use of data, software and/or web tools obtained from the Gravitational Wave Open Science Center (<https://www.gw-openscience.org>), a service of LIGO Laboratory, the LIGO Scientific Collaboration and the Virgo Collaboration. This work was performed on the OzSTAR national facility at Swinburne University of Technology. The OzSTAR program receives funding in part from the Astronomy National Collaborative Research Infrastructure Strategy (NCRIS) allocation provided by the Australian Government. We use the `parallel-Bilby` Bayesian inference software package (Ashton et al. 2019; Smith et al. 2019) with the `Dynesty` nested sampling algorithm (Speagle 2020).

#### REFERENCES

- Aasi, J., Abbott, B. P., Abbott, R., et al. 2015, *Classical and Quantum Gravity*, 32, 074001
- Abbott, B., Abbott, R., Abbott, T., et al. 2017, *PhRvL*, 119, 161101
- Abbott, B. P., Abbott, R., Abbott, T. D., et al. 2017a, *ApJL*, 848, L12
- Abbott, B. P., et al. 2017b, *ApJL*, 850, L39
- . 2019a, *Physical Review X*, 9, 031040
- . 2019b, *Physical Review X*, 9, 011001

- Abbott, B. P., et al. 2020, *ApJL*, 892, L3
- Abbott, R., et al. 2020a, arXiv e-prints, arXiv:2004.08342
- . 2020b, arXiv e-prints, arXiv:2006.12611
- Acernese, F., Agathos, M., Agatsuma, K., et al. 2015, *Classical and Quantum Gravity*, 32, 024001
- Ade, P. A. R., et al. 2016, *A&A*, 594, A13
- Alsing, J., Silva, H. O., & Berti, E. 2018, *MNRAS*, 478, 1377
- Anderson, S. B., Gorham, P. W., Kulkarni, S. R., Prince, T. A., & Wolszczan, A. 1990, *Nature*, 346, 42
- Andrews, J. J., & Mandel, I. 2019, *ApJL*, 880, L8
- Ashton, G., Hübner, M., Lasky, P. D., et al. 2019, *ApJS*, 241, 27
- Bailes, M. 1988, *A&A*, 202, 109
- Belczynski, K., Askar, A., Arca-Sedda, M., et al. 2018, *A&A*, 615, A91
- Bhattacharya, D., & van den Heuvel, E. P. J. 1991, *PhR*, 203, 1
- Biwer, C. M., Capano, C. D., De, S., et al. 2019, *PASP*, 131, 024503
- Bransgrove, A., Levin, Y., & Beloborodov, A. 2018, *MNRAS*, 473, 2771
- Burgay, M., D’Amico, N., Possenti, A., et al. 2003, *Nature*, 426, 531
- Chattopadhyay, D., Stevenson, S., Hurley, J. R., Rossi, L. J., & Flynn, C. 2020, *MNRAS*, 494, 1587
- Dietrich, T., Bernuzzi, S., & Tichy, W. 2017a, *PhRvD*, 96, 121501
- Dietrich, T., Ujevic, M., Tichy, W., Bernuzzi, S., & Brüggmann, B. 2017b, *PhRvD*, 95, 024029
- Dietrich, T., et al. 2019, *PhRvD*, 99, 024029
- Farrow, N., Zhu, X.-J., & Thrane, E. 2019, *ApJ*, 876, 18
- Ferdman, R. D., Stairs, I. H., Kramer, M., et al. 2013, *ApJ*, 767, 85
- . 2014, *MNRAS*, 443, 2183
- Ferdman, R. D., Freire, P. C. C., Perera, B. B. P., et al. 2020, *Nature*, 583, 211
- Fonseca, E., Stairs, I. H., & Thorsett, S. E. 2014, *ApJ*, 787, 82
- Gao, H., Cao, Z., Ai, S., & Zhang, B. 2017, *ApJL*, 851, L45
- Goldreich, P., & Reisenegger, A. 1992, *ApJ*, 395, 250
- Grindlay, J., Portegies Zwart, S., & McMillan, S. 2006, *Nature Physics*, 2, 116
- Hannam, M., Schmidt, P., Bohé, A., et al. 2014, *PhRvL*, 113, 151101
- Hills, J. G. 1983, *ApJ*, 267, 322
- Khan, S., Husa, S., Hannam, M., et al. 2016, *PhRvD*, 93, 044007
- Kramer, M. 1998, *ApJ*, 509, 856
- Landry, P., Essick, R., & Chatziioannou, K. 2020, *PhRvD*, 101, 123007
- Lattimer, J. M., & Prakash, M. 2001, *ApJ*, 550, 426
- Lee, W. H., Ramirez-Ruiz, E., & van de Ven, G. 2010, *ApJ*, 720, 953
- Lynch, R. S., Freire, P. C. C., Ransom, S. M., & Jacoby, B. A. 2012, *ApJ*, 745, 109
- Lyne, A. G., Burgay, M., Kramer, M., et al. 2004, *Science*, 303, 1153
- Mapelli, M., & Giacobbo, N. 2018, *MNRAS*, 479, 4391
- Martinez, J. G., Stovall, K., Freire, P. C. C., et al. 2015, *ApJ*, 812, 143
- Metzger, B. D., Thompson, T. A., & Quataert, E. 2018, *ApJ*, 856, 101
- Neijssel, C. J., Vigna-Gómez, A., Stevenson, S., et al. 2019, *MNRAS*, 490, 3740
- Pankow, C. 2018, *ApJ*, 866, 60
- Pejcha, O., Thompson, T. A., & Kochanek, C. S. 2012, *MNRAS*, 424, 1570
- Phinney, E. S., & Sigurdsson, S. 1991, *Nature*, 349, 220
- Prince, T. A., Anderson, S. B., Kulkarni, S. R., & Wolszczan, A. 1991, *ApJL*, 374, L41
- Romani, R. W. 1990, *Nature*, 347, 741
- Romero-Shaw, I. M., Farrow, N., Stevenson, S., Thrane, E., & Zhu, X.-J. 2020, *MNRAS*, 496, L64
- Schwab, J., Podsiadlowski, P., & Rappaport, S. 2010, *ApJ*, 719, 722
- Siegel, D. M., & Metzger, B. D. 2018, *ApJ*, 858, 52
- Smith, R., Ashton, G., Vajpeyi, A., & Talbot, C. 2019, arXiv e-prints, arXiv:1909.11873
- Speagle, J. S. 2020, *MNRAS*, 493, 3132
- Taam, R. E., & van den Heuvel, E. P. J. 1986, *ApJ*, 305, 235
- Tauris, T. M., Langer, N., & Podsiadlowski, P. 2015, *MNRAS*, 451, 2123
- Tauris, T. M., Kramer, M., Freire, P. C. C., et al. 2017, *ApJ*, 846, 170
- van Leeuwen, J., Kasian, L., Stairs, I. H., et al. 2015, *ApJ*, 798, 118
- Veitch, J., Raymond, V., Farr, B., et al. 2015, *PhRvD*, 91, 042003
- Wysocki, D., O’Shaughnessy, R., Wade, L., & Lange, J. 2020, arXiv e-prints, arXiv:2001.01747
- Ye, C. S., Fong, W.-f., Kremer, K., et al. 2020, *ApJL*, 888, L10
- Zhu, X., Thrane, E., Osłowski, S., Levin, Y., & Lasky, P. D. 2018, *PhRvD*, 98, 043002

## APPENDIX

## A. ALTERNATIVE POSSIBILITIES FOR GW190425

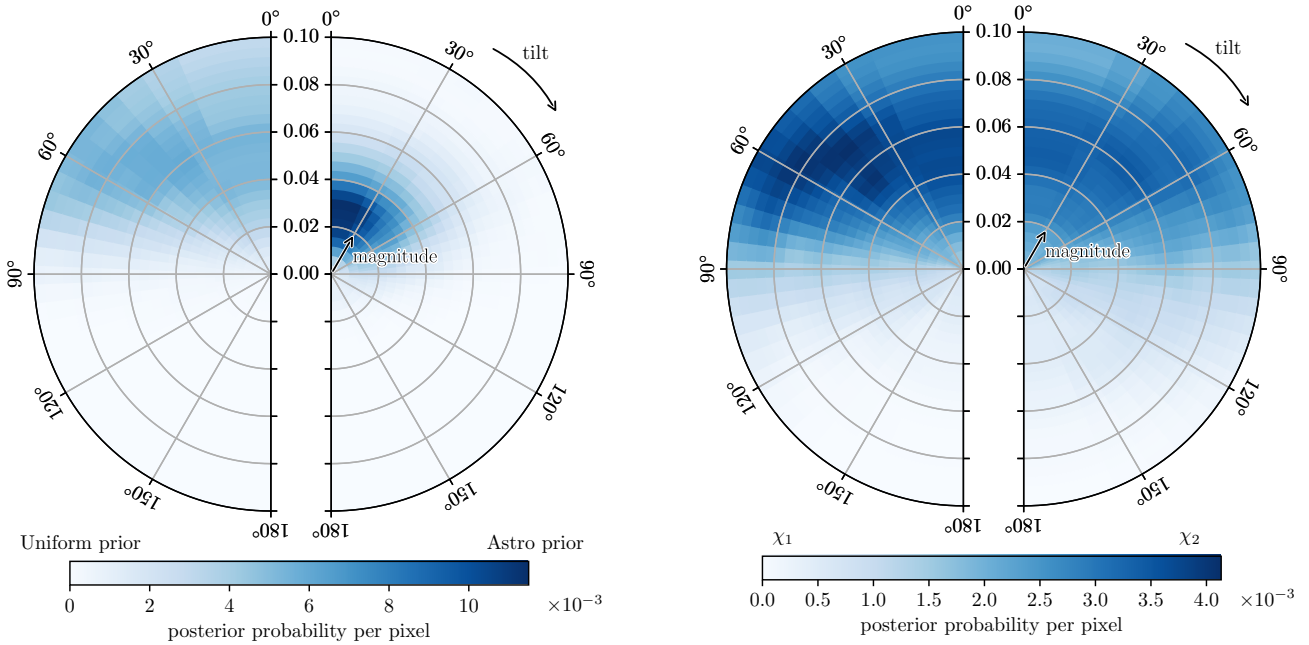


**Figure 5.** Posterior probability densities of NS spins with respect to the orbital angular momentum for GW190425. The left panel is shown for the recycled NS ( $\chi_r$ ), using two different priors, uniform between 0 and 0.1, and the astrophysical prior derived in Section 2. The right panel is shown for component spins  $\chi_1$  and  $\chi_2$ , of the primary and secondary NS, respectively.

Our prior on the recycled NS spin derived in Section 2 only applies to BNS formed through the standard isolated binary evolution channel. In the dynamical formation channel, it is possible that both NS are spinning, or the spinning NS is fully recycled and thus exhibits spins that are disfavoured by our prior<sup>5</sup>. To test these alternative possibilities, we adopt a uniform prior between 0 and 0.1 for the dimensionless spin magnitude  $\chi$ . Here  $\chi = 0.1$  corresponds to a spin period of 3.6 (6.0) ms for a NS radius of 10 (14) km, for  $m = 1.65 M_\odot$ ; Note that PSR 1807–2500B, in the globular cluster NGC 6544, has a spin period of 4.19 ms (Lynch et al. 2012). It is the fastest-spinning recycled pulsar in Galactic BNS systems, but the binary (with an orbital period of 10 days) is not expected to merge within the age of the Universe.

We find a Bayes factor of 2 between the “double-spinning” and “single-spinning” hypothesis for GW190425 (under the same uniform prior for  $\chi$ ), and a Bayes factor of 1.3 between the uniform prior and astrophysical prior for the single-spinning hypothesis. These small Bayes factors imply that the data are insufficient to disentangle these possibilities. It is also worth mentioning that the Bayes factor needs to be weighted by prior odds, which is small for the dynamical BNS formation hypothesis. Figure 5 shows the posterior probability densities for the single-spinning (left) and double-spinning (right) configuration. On the left panel, the left and right half-disk corresponds to the uniform prior and astrophysical prior, respectively. Note that in all cases except the one using the astrophysical prior, each pixel in the plot has equal prior probability. From this test, we conclude that: 1) anti-aligned spins (a tilt angle of  $\sim 180^\circ$ ) are strongly disfavoured; 2) assuming only one NS is spinning, its spin tilt angle is  $\lesssim 60^\circ$ .

<sup>5</sup> If formed through three-body interactions, the captured NS could also be an isolated slow NS. Therefore, the “single-spinning” feature is not unique to the standard formation channel.

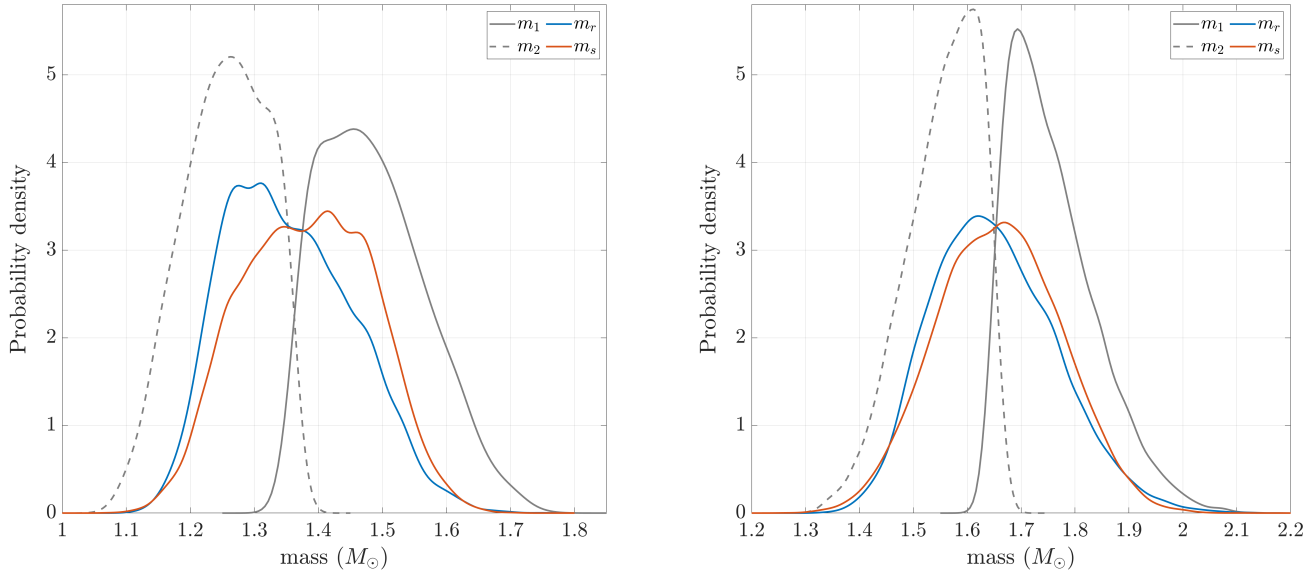


**Figure 6.** Posterior distributions of component masses:  $(m_r, m_s)$  and  $(m_1, m_2)$  for GW170817 (*left*) and GW190425 (*right*). Posteriors of  $(m_1, m_2)$  are taken from the public data release by the LIGO/Virgo collaboration under the low-spin prior (with component spins  $\chi_{1,2} < 0.05$ ). Results are based on the IMRPhenomPv2\_NRTidal waveform model and quoted masses are in the source frame assuming the standard flat  $\Lambda$ CDM cosmology with a Hubble constant  $H_0 = 67.9 \text{ km s}^{-1} \text{ Mpc}^{-1}$  and matter density parameter  $\Omega_m = 0.306$  (Ade et al. 2016).

## B. COMPARISON WITH THE PRIMARY-SECONDARY PARAMETERIZATION

Figure 6 plots the mass measurements obtained in this work, along with the public data release of the LIGO/Virgo collaboration under the primary-secondary parameterization. While not directly comparable, we find our measurements are more constraining:  $(m_r, m_s)$  posteriors are contained inside the envelope spanned by the distributions of  $m_1$  and  $m_2$ . Since BNS mergers are most likely to be of comparable component masses – the most asymmetric merging Galactic BNS is PSR J1913+1102 with  $q = 0.78$  (Ferdman et al. 2020), and the record holder for all BNS (including nonmerging binaries) is PSR J0453+1559 with  $q = 0.75$  (Martinez et al. 2015) – the spin prior proposed in this work enables better characterization of astrophysical BNS with gravitational waves.